

A new air-fuel ratio model fixing the transport delay: Validation and control

Thomas Laurain, Zsófia Lendek, Jimmy Lauber, and Reinaldo M. Palhares

Abstract— Air-fuel ratio control is a crucial problem for engine control since it is one of the most important issues related to pollution reduction. The main difficulty in air-fuel ratio control is the time-varying delay. We propose a new model that includes the delay. This model is identified using real dataset from an engine test bench. The time-varying delay is made constant by using a change of domain. The nonlinearities of the model are handled with the Takagi-Sugeno representation and a linear controller is designed using the Lyapunov direct method. Simulation results highlight the efficiency of the proposed approach compared to classic maps-based controllers.

Keywords: Air-Fuel Ratio; Variable transport delay; crank-angle domain; Takagi-Sugeno representation; Lyapunov-based control design

I. INTRODUCTION

With a continuously growing number of cars, pollution is a crucial matter from an ecological point of view. In the past years, the constraints on pollution imposed by governmental agencies have become tougher and tougher. Current technologies in car industries are mainly based on the three-way catalyst (TWC), which transforms exhaust gases to reduce the emission of NOx, CO₂, and other particles. The TWC has an optimal functioning when the air and the fuel injected into a cylinder are in stoichiometric proportions. To achieve this proportion, an efficient control of the air-fuel ratio (AFR) is needed.

The air-fuel ratio control is challenging due to the fact that the lambda sensor (UEGO sensor) is positioned in the exhaust manifold. Due to this position, the measurement is delayed, the delay depending on the engine speed. Moreover, the sensor is located after the confluence point where the gases from all the cylinders are mixed. This configuration of a unique sensor for several cylinders requires the use of advanced tools, for example [1]. This requires a model that is triggered every engine cycle. This paper proposed a new model in the crankshaft domain with a sampling period of 180 crankshaft degrees. The model is an adaptation of the one presented in [2] with nonlinear gains to capture transient dynamics. It includes the fuel injection timing as well as the control input and the delay. The model is identified based on real datasets from an engine test bench.

Thomas Laurain and Jimmy Lauber are with the LAMIH UMR CNRS 8201, University of Valenciennes, France (e-mail: {thomas.laurain; jimmy.lauber}@univ-valenciennes.fr).

Zsófia Lendek is with the Department of Automation, Technical University of Cluj-Napoca, Romania (e-mail: zsofia.lendek@aut.utcluj.ro).

Reinaldo Palhares is with the Department of Electronics Engineering, Federal University of Minas Gerais, Belo Horizonte, Brazil (e-mail: rpalhares@ufmg.br).

Including the variable transport delay from the cylinder to the lambda sensor allows linking the air-fuel ratio with the mixture that is inside a cylinder. The main problem is that this delay is varying in time because it depends on the engine speed. Furthermore, this variable transport delay can make the control law very complicated and hard to compute for an embedded engine control unit.

That is why many works have investigated advanced controllers without considering any transport delay. For instance, in [3] a fuzzy PID controller is developed. Neural networks based on datasets have been used in several studies, for example [4]–[6] for identification and control, but considering the transport delay as fixed in time. In [7], an adaptive controller is designed considering that the transport delay is known. The adaptive methodology has also been applied in [8] using a mean-value model. [9] has developed a flatness-based controller using a Kalman filter for estimation. However, the delay is considered to be independent of the engine speed.

In those works where the transport delay is considered, it is approximated, identified for compensation or mapped. In [10], a Padé approximation is used to get an analytical expression of the transport delay. In [11], Fourier analysis is used to handle the varying sampling time due to the non-constant engine speed and to model individual cylinder air-fuel ratio. Concerning the variable transport delay, it is taken into account through gain scheduling and integrated into the Fourier coefficients as a map of several operating points. The same method, creating maps for several operating points, has also been used in [12]. They used a collection of LPV controllers for the air-fuel ratio control, and, thanks to the map, the delay is constant at each point. But this mapping method raises the question of transient phases. In the recent work [13] inspired by the study [14], the authors consider the system as an output delay problem. They take into account the transport delay in the augmented state, and they estimate the individual AFR using observers.

As it is illustrated through the literature review, the variable transport delay can be taken into account in the air-fuel ratio control design. Indeed, it can increase performances while ensuring the efficiency even if the engine speed is varying [10]–[14]. This paper presents a transformation to the crankshaft angle domain, where the transport delay becomes constant because it is only depending on values from the past as introduced in [14]. It is possible to take into account the delay if it is known during the AFR controller design. Additionally, the case of idle speed is considered. This is because in hybrid propulsion, the internal combustion engine is often used to reload the battery as a generator group, and it is working at idle speed. Moreover, because the variable transport delay depends on the inverse of the engine speed

(see next section), this delay is maximized at low speed. This is the perfect case to illustrate the interest in the proposed methodology.

This paper first introduces the new air-fuel model and presents its identification and validation in Section 2. Section 3 is dedicated to the transformation to the crank-angle domain so that the transport delay is fixed. Section 4 presents the controller design. Finally, Section 5 gives some simulation results on AFR ratio control with discussions and conclusions.

II. AIR-FUEL RATIO MODEL

A. Continuous-time model

The air-fuel ratio (AFR) represents the ratio between the quantity of injected fuel and injected air inside a cylinder. In order to optimize the functioning of the three-ways catalyst, the quantities should be in stoichiometric proportions, i.e. $\lambda(t)$ should be equal to 1, where

$$\lambda(t) = \frac{m_{air}(t)}{14.67 \times m_{fuel}(t)} \quad (1)$$

where $m_{air}(t)$ and $m_{fuel}(t)$ stand for the amount of air and fuel respectively, and the stoichiometric coefficient is 14.67.

Moreover, considering the dynamics of the lambda sensor, the air-fuel ratio can be modelled as a first-order system. The following model is adapted from [2]:

$$\dot{\lambda}(t) = -\frac{1}{\tau} \lambda(t) + \frac{m_{air}(t-\delta(t))}{14.67 \tau} \times \frac{1}{K_{inj}(t_{inj}(t-\delta(t))-t_0)} \quad (2)$$

where τ is the time constant of the lambda sensor and K_{inj} is the injector constant such that $m_{fuel}(t) = K_{inj} \times t_{inj}(t)$. $t_{inj}(t)$ is the control input and stands for the time of injection (i.e., the time during which the fuel is injected into the cylinder). t_0 is the injection dead time. The three parameters τ , K_{inj} and t_0 are engine coefficients and have to be identified. $\delta(t)$ is the variable transport delay. Even if $\delta(t)$ is time-varying, it does not directly depend on the time but on the crankshaft angle velocity, such that:

$$\delta(t) = \frac{\theta_{fix}}{\dot{\theta}(t)} \quad (3)$$

where θ_{fix} is the length of the delay expressed in crank-angle. For example, it is commonly considered in the literature [2], [15] that the variable transport delay for AFR is equal to two turns of the crankshaft, i.e. $\theta_{fix} = 720$ crankshaft degrees. The idea of this paper is to move from the continuous-time domain to the crank-angle domain in order to obtain a fixed transport delay. $\dot{\theta}(t)$ stands for the angular velocity of the crankshaft in degrees per second and can be converted to the engine speed $n(t)$ in turns per minute:

$\dot{\theta}(t) = \frac{360}{60} n(t)$. With the above considerations, equation (2) can be rewritten as:

$$\dot{\lambda}(t) = -\frac{1}{\tau} \lambda(t) + \frac{1}{14.67 \tau K_{inj}} \times \frac{m_{air} \left(t - \frac{720}{6n(t)} \right)}{\left(t_{inj} \left(t - \frac{720}{6n(t)} \right) - t_0 \right)} \quad (4)$$

where $\{K_{inj}, t_0, \tau\}$ are constant parameters depending on the engine that have to be identified. In this control problem, the time of injection $t_{inj}(t)$ is the input. The amount of air $m_{air}(t)$ is considered as an external input, or a disturbance, since it is controlled by the throttle controller. Indeed, the air controller is responsible for regulating the engine speed around a reference value, and the fuel controller has to maintain the AFR as close to 1 as possible.

B. Model Identification

B.1. Classic model

First of all, since the amount of air is not measured, the identification process uses the air mass flow entering the cylinders $\dot{m}_{air}(t)$, which is measured.

In order to identify the parameters K_{inj} , t_0 and τ in (4), a dataset from the engine test bench located at the LAMIH is used. This test bench is a D4FT 1.2L Renault engine equipped with the same sensors as commercial cars. In the case of AFR control, it means that only the lambda sensor located in the exhaust manifold can be used. The identification is performed using standard methods implemented in the Parameter identification function of the Simulink Design Optimization toolbox. An engine dataset with idle speed (reference at 900rpm) and hot water temperature ($T_w > 75^\circ C$) are first considered.

Even at idle speed, the engine speed is varying around the reference with accuracy depending on the current implemented controller. Moreover, the engine may face external disturbances that can highly affect the engine speed. That is why identifying the model (4) does not provide satisfying results with several methods. Speed-dependent gains should be considered to make the model matching the real data.

B.2. Speed-dependent model

In order to include the speed, two polynomial gains $K_1(n(t))$ and $K_2(n(t))$ are added to the previous model (4). We consider the model:

$$\dot{\lambda}(t) = -\frac{K_2(n(t))}{\tau} \lambda(t) + \frac{K_1(n(t))}{14.67 \tau K_{inj}} \times \frac{\dot{m}_{air} \left(t - \frac{720}{6n(t)} \right)}{\left(t_{inj} \left(t - \frac{720}{6n(t)} \right) - t_0 \right)} \quad (5)$$

These gains are polynomial expressions depending on the engine speed, i.e. $K_1(n(t)) = a_0 + a_1 n(t) + a_2 n^2(t)$ and $K_2(n(t)) = b_0 + b_1 n(t) + b_2 n^2(t)$. The number of parameters that have to be identified increases, however, these polynomial gains are able to capture transient dynamics, as presented in Fig. 1.

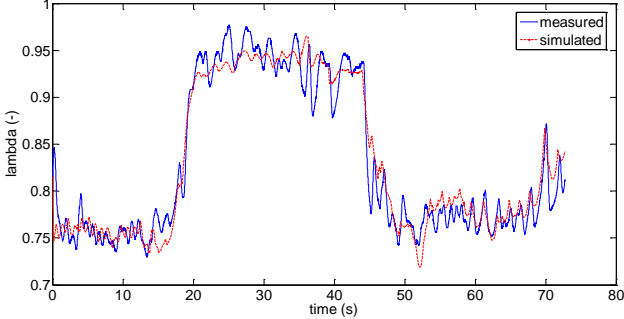


Figure 1. Results of the AFR model identification

The nine parameters have been identified as follows: $\tau = 1.944$, $K_{inj} = 0.2027$, $t_0 = -0.001327$, $a_0 = 9.059$, $a_1 = -0.0188$, $a_2 = 1.0565 \times 10^{-5}$, $b_0 = -1.3482$, $b_1 = 0.002564$ and $b_2 = 3.68 \times 10^{-7}$.

Now that the model parameters have been identified, the engine model is tested with an engine dataset with similar conditions for the speed (idle speed) but with a water temperature continuously increasing in the set $T_w \in [64, 72]$ in Celsius degrees (transient phase for temperature – “tepid”).

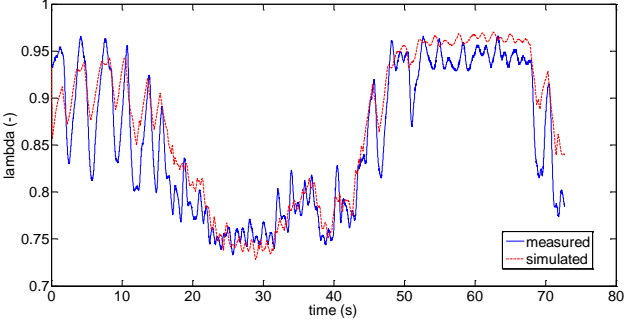


Figure 2. Validation of the AFR model with tepid temperatures

As one can see in Fig. 2, the model is not perfectly accurate in term of amplitude when the water temperature is not hot enough ($t \in [0, 20s]$). If the mean value is reached, the amplitude of the signal is different. This suggests that the model also depends on the temperature.

B.3. Temperature-dependent model

The model can be improved by integrated temperature-dependent coefficients in equation (5). In what follows, the time index is omitted for clarity.

$$\dot{\lambda} = \frac{1+K_w T_w}{\tau} \left(-K_2(n, T_w) \lambda + \frac{K_1(n, T_w) \dot{m}_{air}(t-\delta)}{14.67 K_{inj} t_{inj}(t-\delta)} \right) \quad (6)$$

where K_w is a global gain to be identified, and the polynomial gains are now depending on both the speed and the temperature T_w :

$$\begin{cases} K_1(n, T_w) = a_0 + a_1 n + a_2 n^2 + a_3 T_w + a_4 n T_w \\ K_2(n, T_w) = b_0 + b_1 n + b_2 n^2 + b_3 T_w + b_4 n T_w \end{cases} \quad (7)$$

However, even such a complex model including the water temperature is not valid at low temperatures (around $T_w = 30^\circ C$). Indeed, the behavior of the engine at low temperatures is hard to control, so the currently implemented strategy is mainly based on maps. That is why we focus on normal temperature situations.

The identified model (5) is kept for controller design. The validation presented in Fig. 2 is satisfactory, taking into account that the controller is going to compensate the oscillations. For the rest of the paper, we consider for engine operating conditions that the water temperature is high enough such that the model is valid ($T_w > 70^\circ C$).

III. CRANK-ANGLE DOMAIN MODEL

A. Discrete transformation

The engine is controlled by the electronic control unit (ECU). This device receives signals from the sensors with a certain sampling time, or depending on crankshaft angles. For example, the top-dead center sensor provides a single peak every 180 crankshaft degrees. Therefore, it would be convenient to have a model in the crank-angle domain where the sampling period is expressed as a function of the crank-angle $\theta(t)$ [16], [17]. Moreover, it has been shown in [18] that this angular domain is suitable for engine control. Finally, because the transport delay is depending on the engine speed, in the crank-angle domain, the delay becomes fixed. The idea behind the transformation is to express all the variables and their dynamics using the crankshaft angle θ . The variation of $\lambda(t)$ then becomes:

$$\dot{\lambda}(t) = \frac{d\lambda(t)}{dt} = \frac{d\lambda(t)}{d\theta(t)} \times \frac{d\theta(t)}{dt} \quad (8)$$

The time-derivative of the crankshaft angle $\theta(t)$ is in our case the angular velocity $\dot{\theta}(t)$ [deg/sec] that is related to the engine speed $n(t)$ [turns/min]:

$$\dot{\lambda}(t) = \frac{d\lambda(t)}{dt} = \frac{d\lambda(t)}{d\theta(t)} \times \dot{\theta}(t) = \frac{d\lambda(t)}{d\theta(t)} \times 6n(t) \quad (9)$$

In order to transform the equations from the continuous-time domain to a discrete domain depending on the crankshaft angle, the Euler transformation in angle is used:

$$\frac{d\lambda(t)}{d\theta(t)} = \frac{\lambda^\theta(k+1) - \lambda^\theta(k)}{T_s^\theta} \quad (10)$$

where $\lambda^\theta(k)$ stands for the air-fuel ratio expressed in the crank-angle domain and T_s^θ is the sampling period in

crankshaft degrees, assumed to be small enough such that no information is lost during the transformation. Note that k here denotes the sample index in the crank-angle domain. Then, by combining (9) and (10), we have:

$$\lambda^\theta(k+1) = \lambda^\theta(k) + \frac{T_s^\theta}{6n(k)} \frac{d\lambda^\theta(k)}{dt} \quad (11)$$

Applying (11) on the AFR model (5), we get the model expressed in the crank angle domain:

$$\lambda^{\theta+} = \lambda^\theta - \frac{T_s^\theta K_2(n)}{6\tau n} \lambda + \frac{T_s^\theta K_1(n)}{88.02\tau n K_{inj}} \frac{\dot{m}_{air}(k-\Upsilon(\delta))}{t_{inj}(k-\Upsilon(\delta))-t_0} \quad (12)$$

where the k index is removed for notation, and $\lambda^{\theta+}$ denotes $\lambda^\theta(k+1)$. $\Upsilon(\cdot)$ is a function that converts the delay in seconds into the delay in crank angles. Moreover, using the expression of the delay (3), it stands: $\Upsilon(\cdot) = \dot{\theta}(k)\delta(k) = \theta_{fix}$. In addition, this delay is fixed in the new crank-angle domain, so $\Upsilon(\cdot) = T_s^\theta \times \mu$ with μ the delay in discrete samples (integer). By combining the two expressions, the sampling period in crankshaft degrees can be calculated as:

$$T_s^\theta = \frac{\theta_{fix}}{\mu} \quad (13)$$

The engine has a periodic behavior. Every 180 crankshaft degrees, it enters into a new phase: intake, compression, explosion or exhaust. Then, the sampling period for the crank-angle domain is chosen as $T_s^\theta = 180$. Consequently:

$$\mu = \frac{\theta_{fix}}{T_s^\theta} = \frac{720}{180} = 4 \quad (14)$$

By transforming the continuous model (5) into the crank-angle domain model with a sampling period $T_s^\theta = 180$, the delay becomes fixed and equal to 4 samples. Equation (12) becomes:

$$\lambda^{\theta+} = \lambda^\theta + \frac{T_s^\theta}{6\tau n} \left(-K_2 \lambda + \frac{K_1}{14.67 K_{inj}} \frac{\dot{m}_{air}(k-4)}{t_{inj}(k-4)-t_0} \right) \quad (15)$$

As one can see, the crank-angle model (15) is nonlinear. Instead of using linearization around operating points and maps, this paper proposes to use the Takagi-Sugeno representation. Thanks to this, the stability can be proved not only around operating points, but also during transient phases.

B. Takagi-Sugeno representation

This representation, first introduced by [19], allows dealing directly with the nonlinearities. Indeed, for bounded and measured nonlinearities, it is possible to define a domain in which the Takagi-Sugeno model exactly represents the nonlinear model. The main idea is to build a collection of linear models linked together with nonlinear functions called “membership functions”. More details can be found in [20]. Let us consider equation (15):

$$\lambda^\theta(k+1) = (1 - NL_1(k))\lambda^\theta(k) + NL_2(k)u(k-4) \quad (16)$$

$$\text{with } NL_1(k) = \frac{T_s^\theta K_2(k)}{6\tau n(k)}, \quad NL_2(k) = \frac{T_s^\theta K_1(k)\dot{m}_{air}(k-4)}{6 \times 14.67 \tau K_{inj} n(k)}$$

$$\text{and } u(k-4) = \frac{1}{t_{inj}(k-4)-t_0}.$$

The model (16) can be written as a Takagi-Sugeno state-space representation. It is a SISO system ($x^\theta(k) = \lambda(k)$)

$$x^\theta(k+1) = \sum_{i=1}^r h_i(NL_i(k))(A_i x^\theta(k) + B_i u(k-4)) \quad (17)$$

where $h_i(NL_i(k))$ are the nonlinear functions (membership functions). They verify the property of convex sum, i.e. $\sum_{i=1}^r h_i(NL_i(k)) = 1$. The index r stands for the number of rules. In our case, $r = 4$. For notation purpose, let us denote $\sum_{i=1}^r h_i(NL_i(k))A_i = A_z$. Then, (17) becomes:

$$x^\theta(k+1) = A_z x^\theta(k) + B_z u(k-4) \quad (18)$$

IV. CONTROLLER DESIGN

Once the Takagi-Sugeno model (18) is written, the goal is to design a linear state-feedback controller:

$$u(k) = -F x^\theta(k) \quad (19)$$

The closed-loop is:

$$x^\theta(k+1) = A_z x^\theta(k) - B_z F x^\theta(k-4) \quad (20)$$

and it can be written as:

$$\begin{bmatrix} A_z & -I & -B_z F \end{bmatrix} \begin{bmatrix} x^\theta(k) \\ x^\theta(k+1) \\ x^\theta(k-4) \end{bmatrix} = 0 \quad (21)$$

To prove the stability of the closed-loop system, the direct Lyapunov method is used with the Lyapunov function:

$$V(k) = x^\theta(k)^T P x^\theta(k) + \sum_{i=k-4}^{k-1} x^\theta(i)^T Q x^\theta(i) \quad (22)$$

The difference $\Delta V = V(k+1) - V(k)$ can be written as:

$$\begin{bmatrix} x^\theta(k) \\ x^\theta(k+1) \\ x^\theta(k-4) \end{bmatrix}^T \begin{bmatrix} -P+Q & 0 & 0 \\ 0 & P & 0 \\ 0 & 0 & -Q \end{bmatrix} \begin{bmatrix} x^\theta(k) \\ x^\theta(k+1) \\ x^\theta(k-4) \end{bmatrix} < 0 \quad (23)$$

Using the Finsler lemma [21] on (21) and (23), (23) is satisfied if there exist matrices M_{2zz} and M_3 such as:

$$\begin{bmatrix} 0 \\ M_{2zz}^{-1} \\ M_3^{-1} \end{bmatrix} \begin{bmatrix} A_z & -I & -B_z F \end{bmatrix} + (*) + \begin{bmatrix} -P+Q & 0 & 0 \\ 0 & P & 0 \\ 0 & 0 & -Q \end{bmatrix} < 0 \quad (24)$$

where $(*)$ stands for the symmetric term of the left hand side. Equation (24) can be rewritten as:

$$\begin{bmatrix} -P+Q & (*) & (*) \\ M_{2zz}^{-1}A_z & -M_{2zz}^{-1}-M_{2zz}^{-T}+P & (*) \\ M_3^{-1}A_z & -M_3^{-1}-F^TB_z^TM_{2zz}^{-T} & -M_3^{-1}B_zF+(*)-Q \end{bmatrix} < 0 \quad (25)$$

After applying a congruence with $\text{diag}(X, M_{2zz}, M_3)$ with $X = P^{-1}$, a Schur complement is applied and the change of variables $FQ^{-1} = W$ leads to conditions:

$$\begin{bmatrix} -X & (*) & (*) & (*) & (*) \\ X & -Q^{-1} & (*) & (*) & (*) \\ A_zX & 0 & -M_{2zz} - M_{2zz}^T & (*) & (*) \\ 0 & 0 & M_{2zz}^T & -X & (*) \\ A_zX & 0 & N_{zz} & 0 & H_z \end{bmatrix} < 0 \quad (26)$$

with $N_{zz} = -W^T B_z^T - M_{2zz}^T$ and $H_z = -B_z W + (*) - Q^{-1}$.

Sufficient Linear matrix inequality [22] conditions can be developed using the relaxation of [23]:

$$\begin{cases} \Gamma_{ii} < 0, \quad \forall i \in \{1, \dots, r\} \\ \frac{2}{r-1}\Gamma_{ii} + \Gamma_{ij} + \Gamma_{ji} < 0, \quad \forall i, j \in \{1, \dots, r\}^2, i \neq j \end{cases} \quad (27)$$

with Γ_{ij} being the quantity defined by:

$$\Gamma_{ij} = \begin{bmatrix} -X & (*) & (*) & (*) & (*) \\ X & -Q^{-1} & (*) & (*) & (*) \\ A_iX & 0 & -M_{2ij} - M_{2ij}^T & (*) & (*) \\ 0 & 0 & M_{2ij}^T & -X & (*) \\ A_iX & 0 & N_{ij} & 0 & H_i \end{bmatrix} \quad (28)$$

Then, by solving (27), the gains of the linear controller (19) which stabilizes the closed-loop system (20) can be obtained.

V. SIMULATION RESULTS

The AFR continuous-time model (5), with the engine parameters from Section II, is used for the simulation. The speed and the air mass flow are taken from dataset of the engine test bench, and shown in Fig. 3. Fig.4 presents the variable transport delay according to (3). The controller is designed following the presented methodology. The conditions (27) are solved using Matlab. In addition, a second term is added to reach a constant reference, in our case, $\lambda_{ref} = 1$, using classic state-feedback design methods [24]. The controller gain is:

$$F = -12.7282 \quad (29)$$

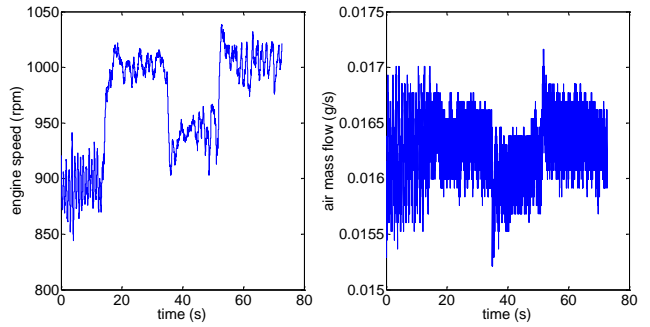


Figure 3. Engine speed and air mass flow considered for the simulation

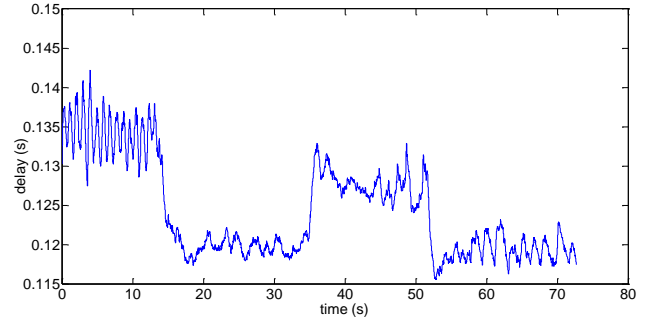


Figure 4. Variable transport delay in seconds

Then, by going to the crank-angle domain, this delay becomes fixed. Fig. 5 presents the results of different control strategies on the air-fuel ratio.

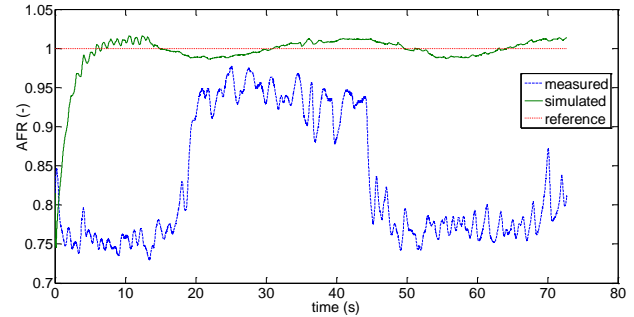


Figure 5. Air-fuel ratio with two different controllers

The dotted red line represents the reference that the controller has to follow, i.e. $\lambda_{ref} = 1$. In green line, the air-fuel ratio obtained using our crank-angle linear controller (19) with the gain (29) is given. In blue discontinuous line, the air-fuel ratio measured on the engine test bench with the current maps-based controller is shown. As one can see, the proposed simple linear state-feedback controller drives the air-fuel ratio to the reference value of 1, ensuring that the three-way catalyst is working in the optimal conditions. Fig. 6 presents the command generated by our new controller as the time of injection is triggered every 180 crankshaft degrees $t_{inj}^\theta(k)$.

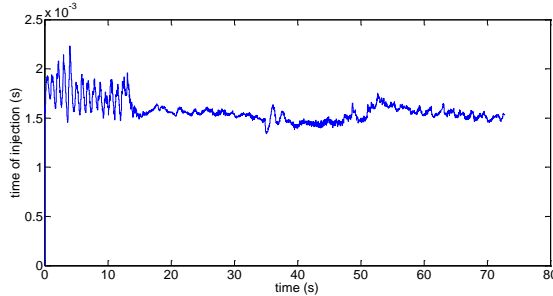


Figure 6. Command of the injectors

VI. CONCLUSION

This paper has presented a new air-fuel ratio model. The classic one from the literature, including a variable transport delay, has been improved using nonlinear gains whose parameters have been identified using real data from the engine test bench. Then, this model has been converted into the crank-angle domain where the transport delay becomes fixed and expressed as a number of samples. The nonlinear behavior has been handled using the Takagi-Sugeno representation. A linear controller has been designed using the Lyapunov direct method to maintain the air-fuel ratio at the reference value. Finally, the simulation results have highlighted the strength of the approach compared to traditional maps-based controllers. Future works will be dedicated to the implementation of the controller on the engine test bench, providing real-time results.

ACKNOWLEDGMENT

This research is sponsored by the International Campus on Safety and Intermodality in Transportation, the Hauts-de-France Region, the European Community, the Regional Delegation for Research and Technology, the Ministry of Higher Education and Research, and the French National Center for Scientific Research (CNRS). This work was also supported by a grant of the Romanian National Authority for Scientific Research and Innovation, CNCS -- UEFISCDI, project number PN-II-RU-TE-2014-4-0942, contract number 88/01.10.2015 and the Brazilian National Research Council (CNPq).

REFERENCES

- [1] S. Bittanti and P. Colaneri, ‘Invariant representations of discrete-time periodic systems’, *Automatica*, vol. 36, no. 12, pp. 1777–1793, 2000.
- [2] J. Lauber, T. M. Guerra, and M. Dambrine, ‘Air-fuel ratio control in a gasoline engine’, *International Journal of Systems Science*, vol. 42, no. 2, pp. 277–286, 2011.
- [3] A. Ghaffari, A. H. Shamekhi, A. Saki, and E. Kamrani, ‘Adaptive fuzzy control for air-fuel ratio of automobile spark ignition engine’, *World Academy of Science, Engineering and Technology*, vol. 48, pp. 284–292, 2008.
- [4] S. W. Wang, D. L. Yu, J. B. Gomm, G. F. Page, and S. S. Douglas, ‘Adaptive neural network model based predictive control for air-fuel ratio of SI engines’, *Engineering Applications of Artificial Intelligence*, vol. 19, no. 2, pp. 189–200, Mar. 2006.
- [5] I. Arsie, C. Pianese, and M. Sorrentino, ‘A procedure to enhance identification of recurrent neural networks for simulating air-fuel ratio dynamics in SI engines’, *Engineering Applications of Artificial Intelligence*, vol. 19, no. 1, pp. 65–77, Feb. 2006.
- [6] Y.-J. Zhai and D.-L. Yu, ‘Neural network model-based automotive engine air/fuel ratio control and robustness evaluation’, *Engineering Applications of Artificial Intelligence*, vol. 22, no. 2, pp. 171–180, Mar. 2009.
- [7] Y. Yildiz, A. M. Annaswamy, D. Yanakiev, and I. Kolmanovsky, ‘Spark ignition engine fuel-to-air ratio control: An adaptive control approach’, *Control Engineering Practice*, vol. 18, no. 12, pp. 1369–1378, Dec. 2010.
- [8] X. Jiao and T. Shen, ‘Lyapunov-design of adaptive air-fuel ratio control for gasoline engines based on mean-value model’, in *Chinese Control Conference (CCC)*, Yantai, China, 2011, pp. 6146–6150.
- [9] G. Rigatos, P. Siano, and I. Arsie, ‘Flatness-based embedded control of air-fuel ratio in combustion engines’, in *International Conference of Computational Methods in Sciences and Engineering (ICCMSE)*, Athens, Greece, 2014, pp. 251–259.
- [10] R. A. Zope, J. Mohammadpour, K. M. Grigoriadis, and M. Franchek, ‘Air-fuel ratio control of spark ignition engines with TWC using LPV techniques’, in *ASME Dynamic Systems and Control Conference*, Hollywood, USA, 2009, pp. 897–903.
- [11] W. Schick, C. Onder, and L. Guzzella, ‘Individual Cylinder Air-Fuel Ratio Control Using Fourier Analysis’, *IEEE Transactions on Control Systems Technology*, vol. 19, no. 5, pp. 1204–1213, Sep. 2011.
- [12] M. Postma and R. Nagamune, ‘Air-Fuel Ratio Control of Spark Ignition Engines Using a Switching LPV Controller’, *IEEE Transactions on Control Systems Technology*, vol. 20, no. 5, pp. 1175–1187, Sep. 2012.
- [13] C. Wang and Z. Liu, ‘Estimation of Individual Cylinder Air-Fuel Ratio in Gasoline Engine with Output Delay’, *Journal of Sensors*, vol. 2016, pp. 1–9, 2016.
- [14] B. He, T. Shen, J. Kako, and M. Ouyang, ‘Input Observer-Based Individual Cylinder Air-Fuel Ratio Control: Modelling, Design and Validation’, *IEEE Transactions on Control Systems Technology*, vol. 16, no. 5, pp. 1057–1065, Sep. 2008.
- [15] E. Hendricks and J. Luther, ‘Model and Observer Based Control of Internal Combustion Engines’, in *International Workshop on Modeling Emissions and Control in Automotive Engines (MECA)*, Salerno, Italy, 2001.
- [16] P. A. Hazell and J. O. Flower, ‘Discrete modelling of spark-ignition engines for control purposes’, *International Journal of Control*, vol. 13, no. 4, pp. 625–632, 1971.
- [17] B. K. Powell, J. A. Cook, and J. W. Grizzle, ‘Modeling and Analysis of an Inherently Multi-Rate Sampling Fuel Injected Engine Idle Speed Control Loop’, in *IEEE American Control Conference (ACC)*, Minneapolis, USA, 1987, pp. 1543–1548.
- [18] S. Yurkovich and M. Simpson, ‘Comparative analysis for idle speed control: A crank-angle domain viewpoint’, in *IEEE American Control Conference (ACC)*, Albuquerque, NM, USA, 1997, pp. 278–283.
- [19] T. Takagi and M. Sugeno, ‘Fuzzy identification of systems and its applications to modeling and control’, *IEEE Transactions on Systems, Man and Cybernetics, Part B (Cybernetics)*, no. 1, pp. 116–132, 1985.
- [20] K. Tanaka and H. O. Wang, *Fuzzy control systems design and analysis: a linear matrix inequality approach*. New York: Wiley, 2001.
- [21] M. C. de Oliveira and R. E. Skelton, ‘Stability tests for constrained linear systems’, in *Perspectives in robust control*, vol. 268, Springer London, 2001, pp. 241–257.
- [22] S. Boyd, L. El Ghaoui, E. Feron, and V. Balakrishnan, *Linear matrix inequalities in system and control theory*, Studies in Applied Mathematics., vol. 15. Society for Industrial and Applied Mathematics (SIAM), 1994.
- [23] H. D. Tuan, P. Apkarian, T. Narikiyo, and Y. Yamamoto, ‘Parameterized linear matrix inequality techniques in fuzzy control system design’, *IEEE Transactions on Fuzzy Systems*, vol. 9, no. 2, pp. 324–332, 2001.
- [24] H. Khalil, *Nonlinear Systems*. New Jersey: Prentice Hall, 1996.